BMED436 Medical Robot
2018250064 Sibeen Kim

Feedback Control

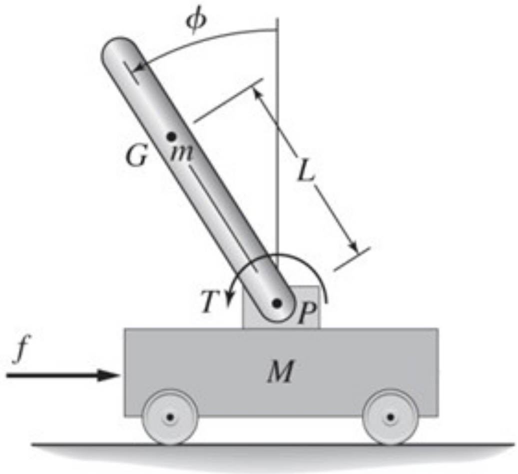

Figure 1: Inverted pendulum system.

Figure 1 illustrates an inverted pendulum system, which consists of a cart capable of moving along a horizontal axis and a pendulum attached to the cart that swings freely. The dynamics of this system are inherently unstable, as the pendulum tends to fall away from its upright position under the influence of gravity. To stabilize the system, a control mechanism must apply appropriate forces to the cart, ensuring the pendulum remains balanced at the upright position while minimizing the cart's movement.

The system parameters are as follows: the mass of the cart $M = 1\,\mathrm{kg}$, the mass of the pendulum $m = 0.3\,\mathrm{kg}$, the moment of inertia of the pendulum about its center of mass $I_G = 0.006\,\mathrm{kg \cdot m^2}$, the length of the pendulum $L = 0.4\,\mathrm{m}$, and the acceleration due to gravity $g = 9.8\,\mathrm{m/s^2}$. These known values form the basis for deriving the equations of motion and designing the control system. The primary challenge lies in stabilizing the pendulum at its upright equilibrium position while simultaneously controlling the cart's position to prevent excessive displacement.

1 System modeling

1.1 Equations of motion

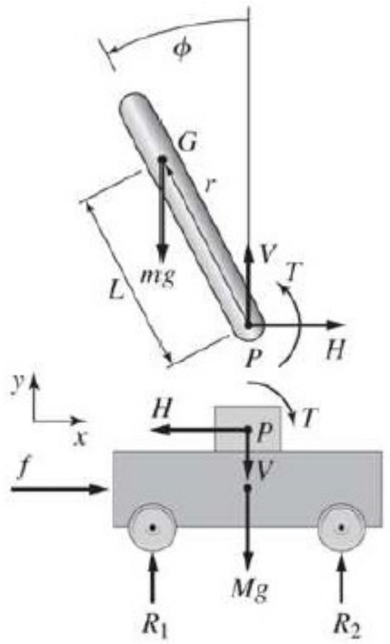

Figure 2: Free body diagram.

Let $(x_P, y_P) = (x, 0)$. Then, $(x_G, y_G) = (x - L\sin\phi, L\cos\phi)$, and the equations of motion for the system can be derived using the free body diagram shown in Figure 2.

Horizontal force on the pendulum:

$$\begin{aligned}
m\ddot{x}_G &= H \\
m\ddot{x}_G &= m\ddot{x} + mL\sin\phi(\dot{\phi})^2 - mL\cos\phi\ddot{\phi} \\
&\approx m\ddot{x} - mL\ddot{\phi} \quad \text{(for small } \phi, \dot{\phi}) \\
H &= m\ddot{x} - mL\ddot{\phi} \qquad (1)
\end{aligned}$$

Vertical force on the pendulum:

$$
\begin{aligned}
m\ddot{y}_G &= V - mg \\
m\ddot{y}_G &= -mL\cos\phi(\dot{\phi})^2 - mL\sin\phi\ddot{\phi} \\
&\approx -mL\phi\ddot{\phi} \quad \text{(for small } \phi, \dot{\phi}) \\
V &= mg - mL\phi\ddot{\phi} \qquad (2)
\end{aligned}
$$

Moment equation for the pendulum:

$$
\begin{aligned}
I_G\ddot{\phi} &= T + VL\sin\phi + HL\cos\phi \\
&\approx VL\phi + HL \quad \text{(for small } \phi) \\
&= (mgL - mL^2\phi\ddot{\phi})\phi + mL\ddot{x} - mL^2\ddot{\phi} \quad \text{(from (1), (2))} \\
&\approx mgL\phi + mL\ddot{x} - mL^2\ddot{\phi} \quad \text{(for small } \phi) \\
0 &= (I_G + mL^2)\ddot{\phi} - mgL\phi - mL\ddot{x}
\end{aligned}
$$

Horizontal force on the cart:

$$
\begin{aligned}
M\ddot{x}_P &= f - H \\
M\ddot{x} &= f - (m\ddot{x} - mL\ddot{\phi}) \quad \text{(from (1))} \\
0 &= (M + m)\ddot{x} - mL\ddot{\phi} - f
\end{aligned}
$$

Equations of motion:

$$
(M + m)\ddot{x} - mL\ddot{\phi} - f = 0 \qquad (3)
$$

$$
(I_G + mL^2)\ddot{\phi} - mgL\phi - mL\ddot{x} = 0 \qquad (4)
$$

1.2 Transfer function

From (4):

$$
\begin{aligned}
mLs^2X(s) &= \{(I_G + mL^2)s^2 - mgL\}\Phi(s) \\
\frac{X(s)}{\Phi(s)} &= \frac{(I_G/mL + L)s^2 - g}{s^2} \qquad (5)
\end{aligned}
$$

From (3), (5):

$$\begin{aligned} mLs^2\Phi(s) &= (M+m)s^2X(s) - F(s) \\ \frac{\Phi(s)}{F(s)} &= \frac{q}{s^2 - q(M+m)g} \\ \text{where} \quad q &= \frac{1}{(M+m)I_G/mL + ML} > 0 \end{aligned} \tag{6}$$

PD controller:

$$\frac{F(s)}{\Phi_d(s) - \Phi(s)} = k_P + k_D s \tag{7}$$

From (6), (7):

$$\begin{aligned} \frac{\Phi(s)}{\Phi_d(s) - \Phi(s)} &= \frac{q(k_P + k_D s)}{s^2 - q(M+m)g} \\ \therefore \frac{\Phi(s)}{\Phi_d(s)} &= \frac{q(k_P + k_D s)}{s^2 + qk_D s + q\{k_P - (M+m)g\}} \end{aligned} \tag{8}$$

2 Routh–Hurwitz stability criterion

To stabilize the inverted pendulum, we analyze the characteristic equation of the system transfer function, $\frac{\Phi(s)}{\Phi_d(s)}$, given by:

$$P(s) = s^2 + qk_D s + q\{k_P - (M+m)g\} = 0. \tag{9}$$

For a second-order polynomial, the Routh–Hurwitz stability criterion states that all roots will have negative real parts (stability) if and only if all coefficients of the polynomial are positive. Applying this condition to $P(s)$, we obtain:

$$qk_D > 0 \quad \text{and} \quad q\{k_P - (M+m)g\} > 0.$$

Since $q > 0$, these reduce to:

$$k_D > 0 \quad \text{and} \quad k_P > (M+m)g.$$

Thus, for the inverted pendulum to remain stable, the proportional gain k_P must exceed the critical value $(M+m)g$, and the derivative gain k_D must be positive.

3 Impulse response

The damping ratio ζ and natural frequency ω_n of the system are defined by the standard second-order characteristic equation:

$$P(s) = s^2 + 2\zeta\omega_n s + \omega_n^2.$$

From the system's characteristic equation (9), we have:

$$\begin{aligned} 2\zeta\omega_n &= qk_D, \\ \omega_n^2 &= q\{k_P - (M+m)g\}. \end{aligned}$$

Thus, the damping ratio can be expressed as:

$$\zeta = \frac{1}{2}k_D\sqrt{\frac{q}{k_P - (M+m)g}}.$$

Given the desired damping ratio $\zeta \approx \frac{1}{2}$,

$$k_D = \sqrt{\frac{k_P - (M+m)g}{q}}. \tag{10}$$

Here, we choose k_P as the primary tuning parameter, and k_D is computed by (10) to satisfy the desired damping ratio. Once the gains are selected, the impulse response of the system can be analyzed to validate the design.

```
M = 1; m = 0.3; I_G = 0.006; L = 0.4; g = 9.8;
q = 1/((M+m)*I_G/(m*L)+M*L);
t = 0:0.01:10;

k_P = 25; % k_P > (M+m)*g, tune this!
k_D = sqrt((k_P-(M+m)*g)/q); % k_D > 0, damping ratio = 0.5

numerator = [q*k_D, q*k_P];
denominator = [1, q*k_D, q*(k_P-(M+m)*g)];
feedback_control_system = tf(numerator, denominator);

y = impulse(feedback_control_system, t);
```

Listing 1: Impulse response in MATLAB.

Listing 1 provides the MATLAB code used to compute the impulse response, and the animation for varying k_P is provided in `[link]`. Figure 3 shows the impulse responses for the system with $k_P = 20$, $k_P = 25$, and $k_P = 30$.

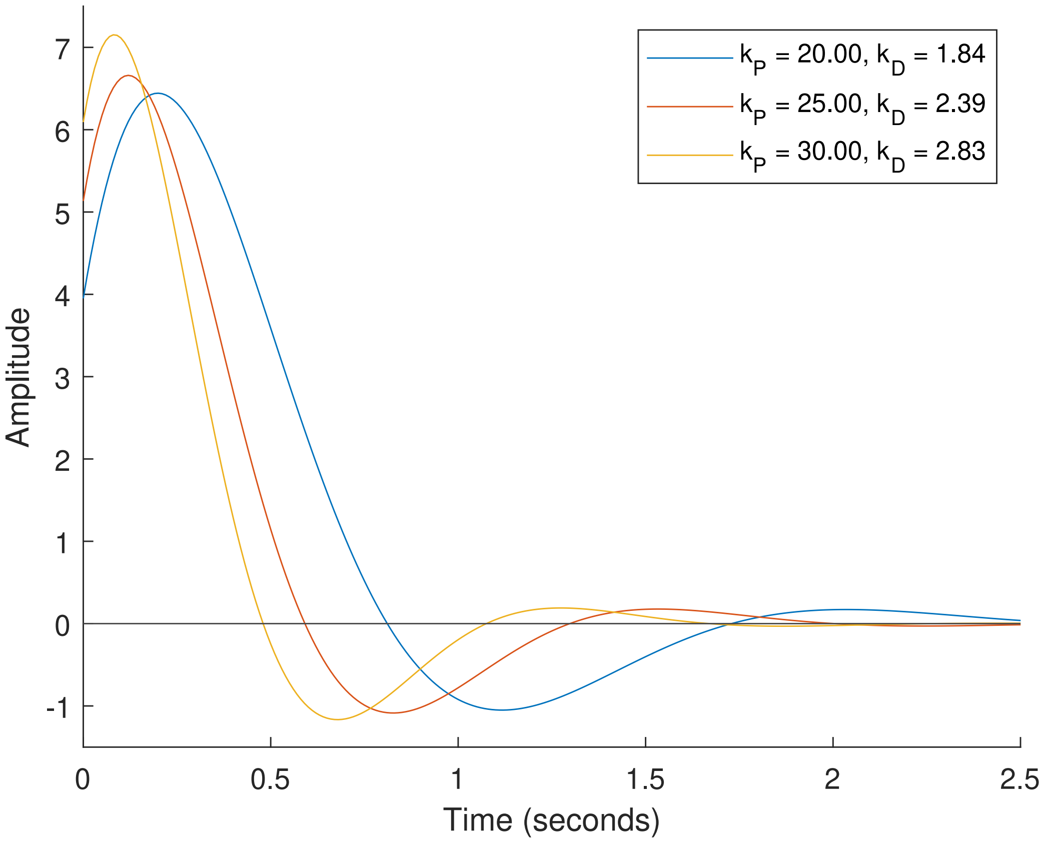

Figure 3: Impulse response for $k_P = 20$, 25, and 30.

The response for $k_P = 20$ exhibits a relatively long settling time, indicating low responsiveness and slow convergence to the equilibrium position. For $k_P = 30$, the system response shows relatively high overshoot before stabilizing. In contrast, the response for $k_P = 25$ achieves a balance between settling time and overshoot. Based on this analysis, we chose $(k_P, k_D) = (25, 2.39)$.

4 Time Response Analysis

4.1 Simulink Implementation

In this section, we analyze the time response of the system under the initial condition $\phi(0) = -10°$. The system is implemented in Simulink based on the transfer functions derived in previous sections.

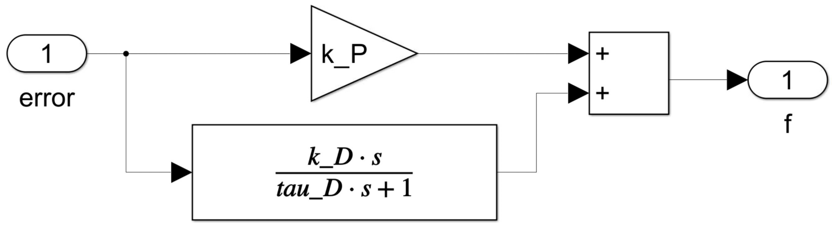

Figure 4: PD Controller.

Figure 4 represents the PD controller implemented in Simulink. Unlike the theoretical expression in equation (7), where the PD controller is $K_P + K_D s$, here it is implemented as $K_P + \frac{K_D s}{\tau_D s+1}$. For practical reasons, a pole with a short time constant τ_D is added to the PD controller. The pole helps limit the loop gain at high frequencies, which is desirable for disturbance rejection.

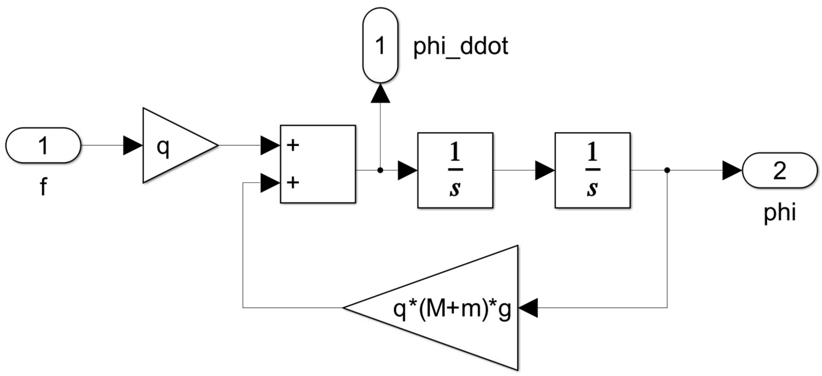

Figure 5: Plant Φ.

Figure 5 shows the plant for $\Phi(s)$, derived in equation (6). This block represents the plant dynamics of the pendulum's angular displacement.

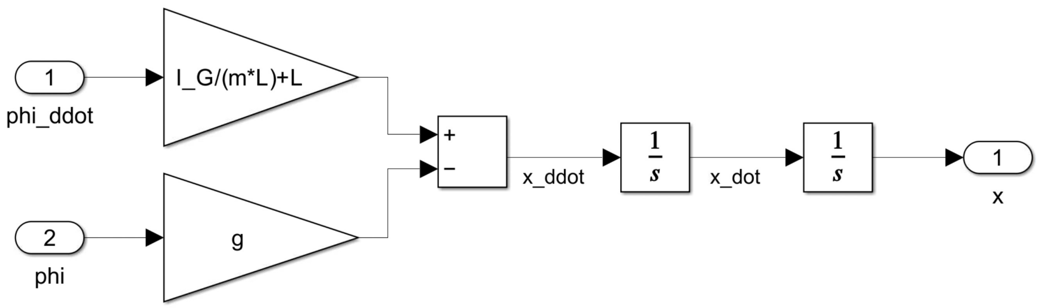

Figure 6: Plant X.

Figure 6 shows the plant for $X(s)$, derived in equation (5). This block models the dynamics of the cart's displacement.

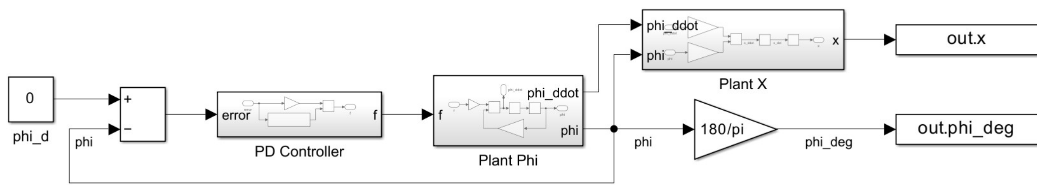

Figure 7: Overall system.

Finally, Figure 7 combines the individual components to represent the entire control system implemented in Simulink.

4.2 Time Response: $\phi(t)$

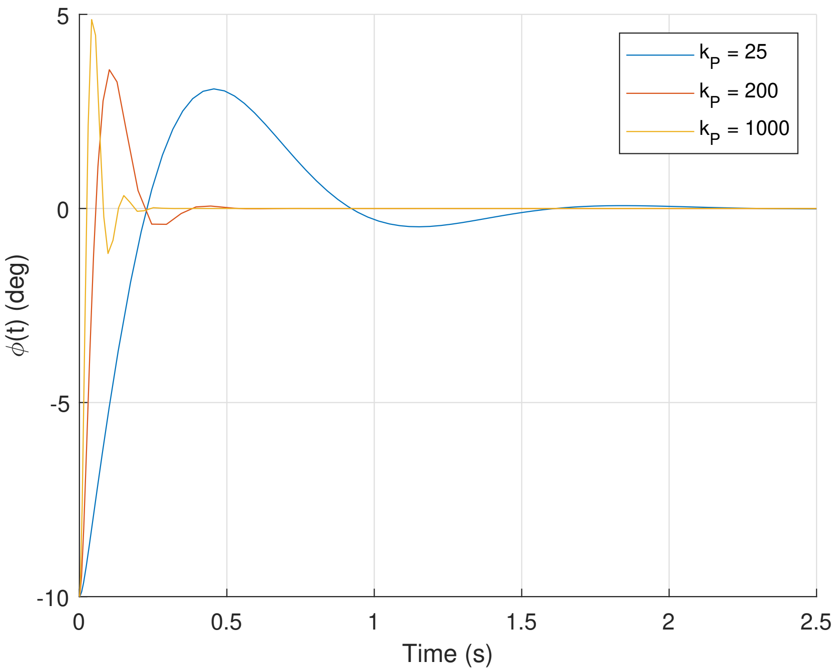

Figure 8: Time response of $\phi(t)$ for $k_P = 25$, 200, and 1000.

Figure 8 shows the time response of $\phi(t)$ for different values of k_P: 25, 200, and 1000. The observed trends are consistent with the previous impulse response analysis (Figure 3). As k_P (and consequently k_D) increases, the response becomes faster but exhibits increased overshoot. For $k_P = 25$, the response is relatively slow but exhibits no significant overshoot. On the other hand, $k_P = 200$ and $k_P = 1000$ show faster responses but larger overshoots, with $k_P = 1000$ displaying the highest overshoot.

4.3 Time Response: $x(t)$

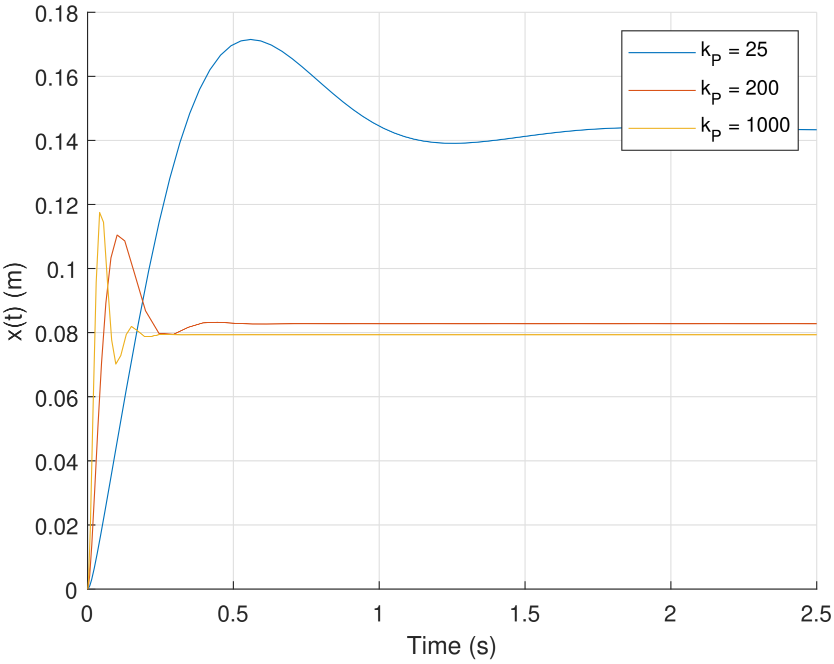

Figure 9: Time response of $x(t)$ for $k_P = 25$, 200, and 1000.

Figure 9 illustrates the time response of $x(t)$ for the same setup. For $k_P = 25$, the cart exhibits the worst performance, with an initial peak displacement of approximately 0.17 m and a steady-state displacement exceeding 0.14 m. For $k_P = 200$ and $k_P = 1000$, the steady-state displacement converges to around 0.08 m, with $k_P = 200$ being slightly higher. However, the initial peak is about 0.11 m for $k_P = 200$, while it rises to 0.12 m for $k_P = 1000$.

This analysis suggests that increasing k_P provides diminishing benefits in terms of steady-state displacement while increasing the initial overshoot. Based on these results, $k_P = 200$ represents a balanced choice that minimizes cart movement while ensuring acceptable pendulum stabilization.

Animations of the inverted pendulum time responses are available for [$k_P = 25$], [$k_P = 200$], and [$k_P = 1000$].

To minimize cart movement, one approach would be to introduce a position feedback term in the controller design. Alternatively, tuning k_P to avoid excessive overshoot, as observed for $k_P = 1000$, is critical for achieving both pendulum stabilization and limited cart displacement.